

## Supplementary Materials

# Exploring Conformational Landscapes and Binding Mechanisms of Convergent Evolution for the SARS-CoV-2 Spike Omicron Variant Complexes with the ACE2 Receptor Using AlphaFold2-Based Structural Ensembles and Molecular Dynamics Simulations

Nishank Raisinghani,<sup>1</sup> Mohammed Alshahrani,<sup>1</sup> Grace Gupta,<sup>1</sup> Sian Xiao<sup>3</sup>, Peng Tao<sup>3</sup>,  
Gennady Verkhivker<sup>1,2\*</sup>

<sup>1</sup>Keck Center for Science and Engineering, Graduate Program in Computational and Data Sciences, Schmid College of Science and Technology, Chapman University, Orange, CA 92866, United States of America

<sup>2</sup> Department of Biomedical and Pharmaceutical Sciences, Chapman University School of Pharmacy, Irvine, CA 92618, United States of America

<sup>3</sup>Department of Chemistry, Center for Research Computing, Center for Drug Discovery, Design, and Delivery (CD4), Southern Methodist University, Dallas, Texas, 75275, United States of America

\* Correspondence: verkhivk@chapman.edu; Tel.: +1-714-516-4586 (G.V)

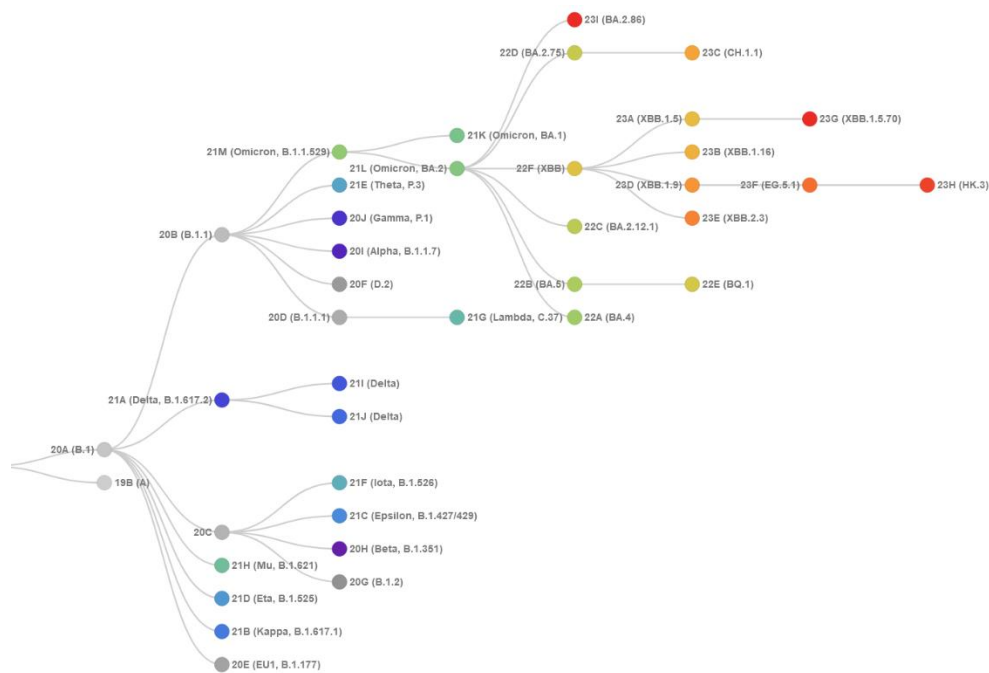


**Figure S1.** The evolutionary tree of current SARS-CoV-2 clades. XBB.1, XBB.1.5 and XBB.1.5.70 variants are shown on the current tree. The graph is generated using Nextstrain, an open-source project for real time tracking of evolving pathogen populations (<https://nextstrain.org/>).

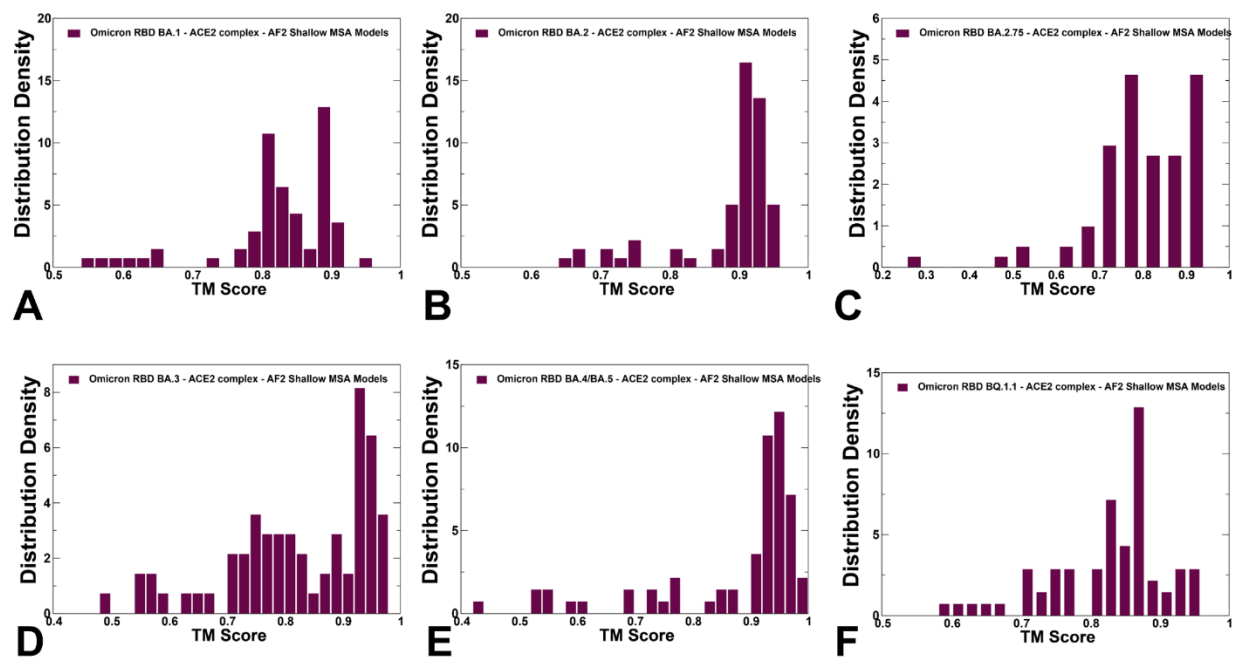


**Figure S2.** The density distribution of TM-score measuring structural similarity of the AF2-MSA shallow depth predicted ensembles with respect to the experimental structures. The density distribution of the TM-scores for BA.1 (A) BA.2 (B), BA.2.75 (C), BA.3 (D), BA.4/BA.5 (E) and BQ.1.1 (F). The density distributions are shown in maroon-colored filled bars.

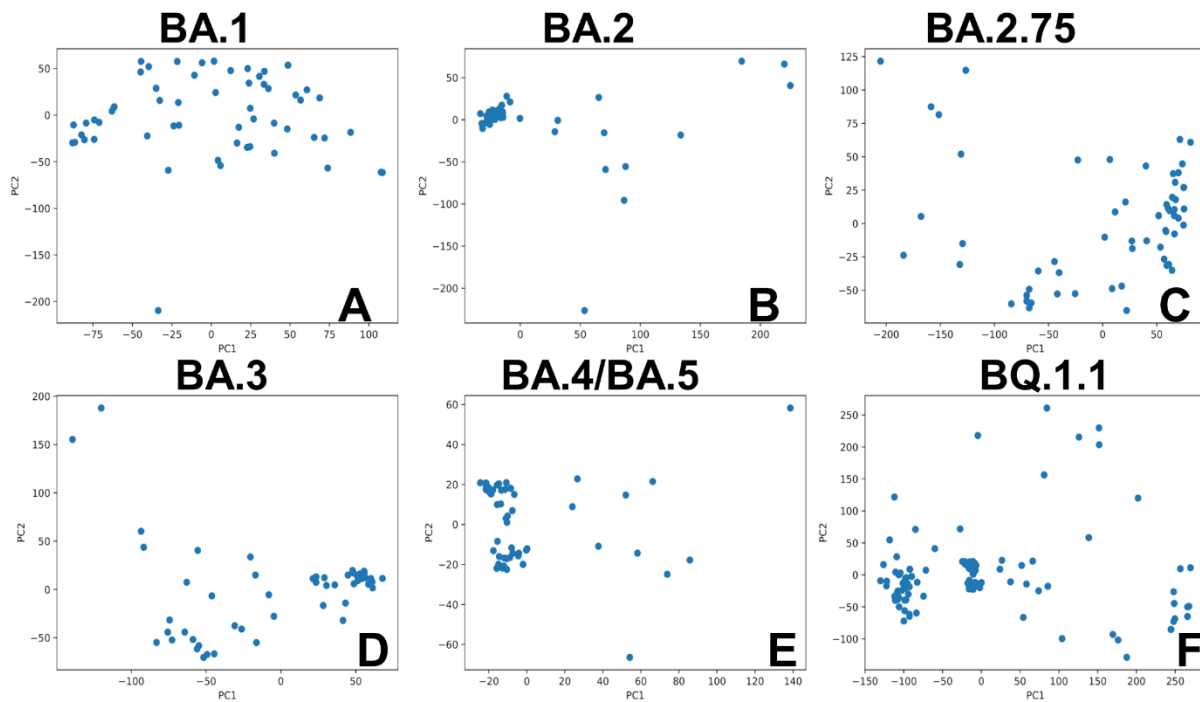


**Figure S3.** PCA of the AF2-generated ensembles for the Omicron RBD-ACE2 complexes using shallow MSA subsampling. PCA graphs are shown for the BA.1 RBD-ACE2 complex (A), BA.2 RBD-ACE2 complex (B), BA.2.75 RBD-ACE2 complex (C), BA.3 RBD-ACE2 complex (D), BA.4/BA.5 RBD-ACE2 complex (E), and BQ.1.1 RBD-ACE2 complex (F).

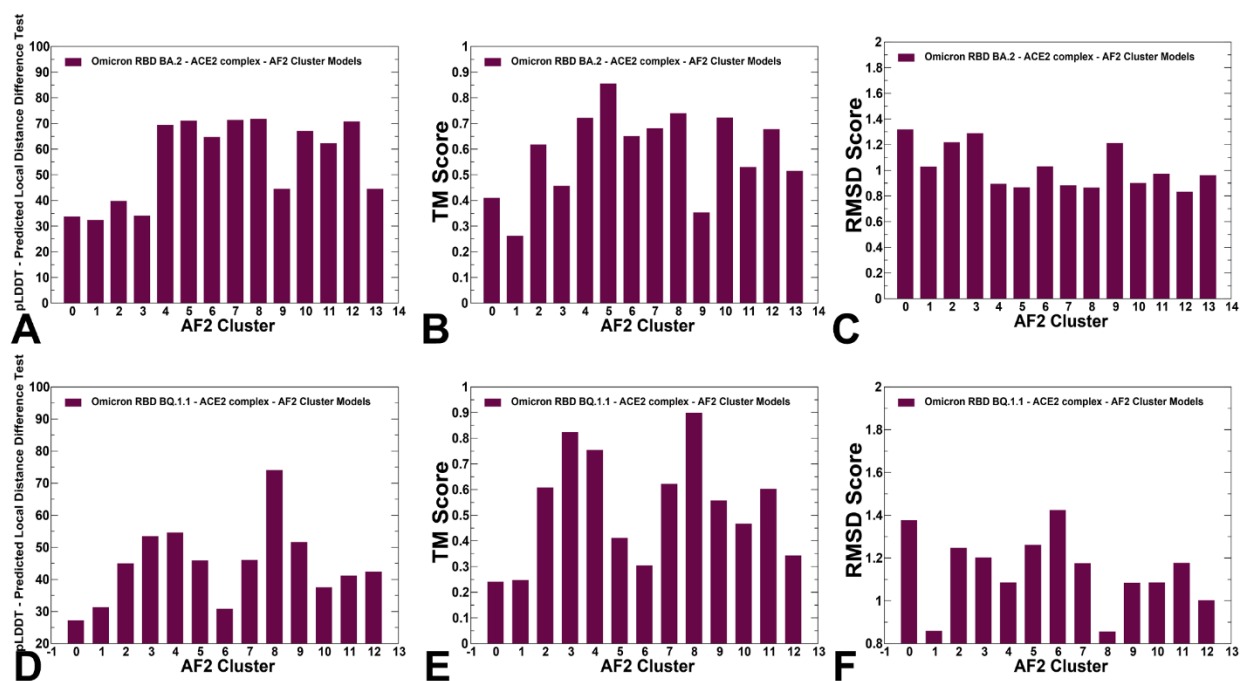


**Figure S4.** The distribution of statistical confidence pLDDT and structural similarity metrics for conformational cluster conformations obtained from AF-Cluster. The pLDDT profile as a function of cluster number from AF-Cluster predictions for BA.2 RBD-ACE2 complex (A) an BQ1.1 RBD-ACE2 complex (D). The TM-core profile as a function of cluster number from AF-Cluster predictions for BA.2 RBD-ACE2 complex (B) an BQ1.1 RBD-ACE2 complex (E). The RMSD from the experimental structure profile as a function of cluster number from AF-Cluster predictions for BA.2 RBD-ACE2 complex (C) an BQ1.1 RBD-ACE2 complex (F).

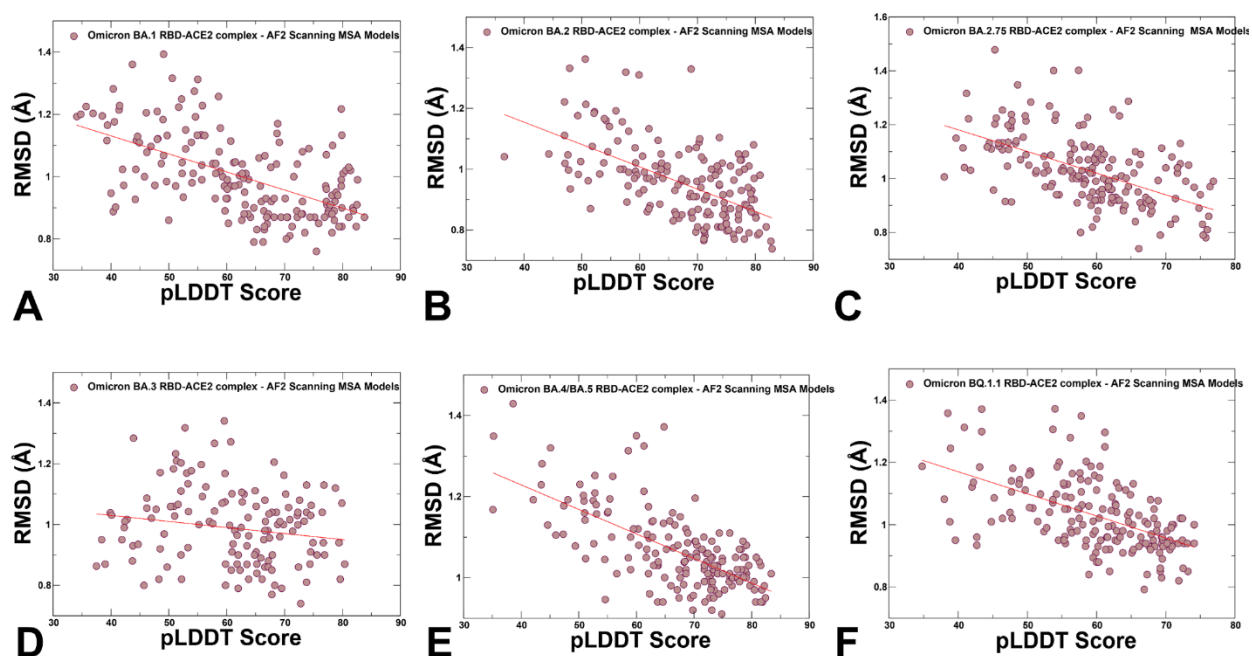


**Figure S5.** The scatter plots between the pLDDT scores and RMSD scores for the conformational ensembles obtained using AF2 adaptation with randomized sequence scanning and subsequent shallow MSA subsampling. The scatter plot distributions are shown for structural ensembles obtained for BA.1 (A) BA.2 (B), BA.2.75 (C), BA.3 (D), BA.4/BA.5 (E) and BQ.1.1 (F). The density distributions are depicted as brown-colored filled circles.

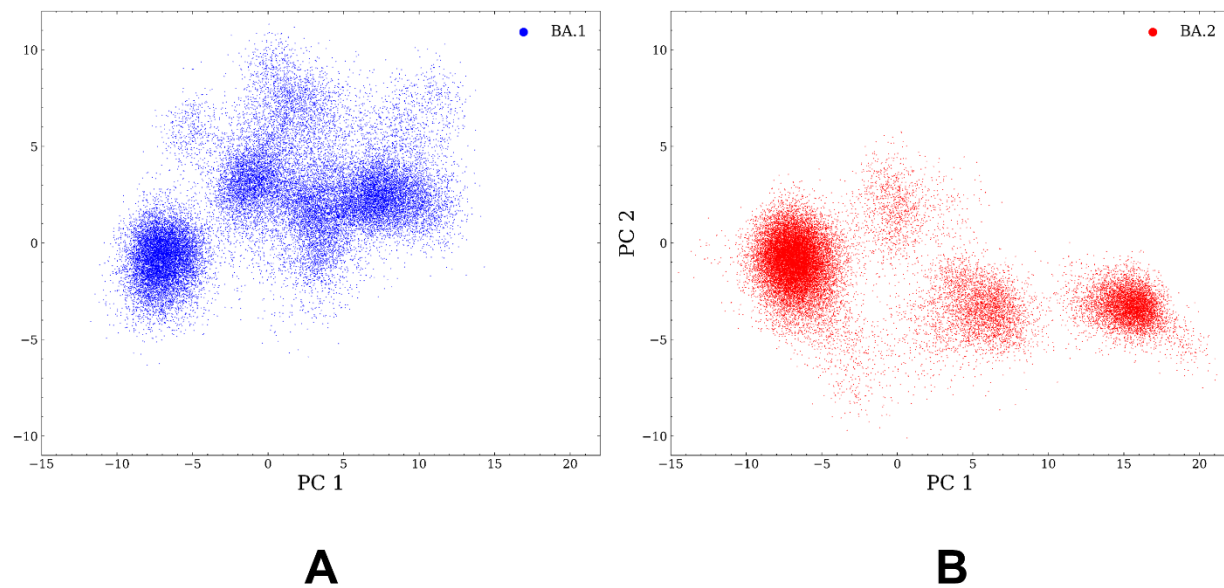


**Figure S6.** PCA of the conformational ensembles obtained from MD simulation trajectories for the BA.1 RBD-ACE2 complex (A) and BA.2 RBD-ACE2 complex (B).